frontiers | Frontiers in Energy Research

TYPE Original Research
PUBLISHED 09 November 2022
DOI 10.3389/fenrg.2022.1041900

OPEN ACCESS

EDITED BY
Songbai Cheng,
Sun Yat-sen University, China

REVIEWED BY
Xingkang Su,
Lanzhou University, China
Kai Wang,
Sun Yat-sen University, China

*CORRESPONDENCE
Zhigang Zhang,
zg_zhang@hrbeu.edu.cn

SPECIALTY SECTION
This article was submitted to Nuclear Energy, a section of the journal Frontiers in Energy Research

RECEIVED 11 September 2022
ACCEPTED 24 October 2022
PUBLISHED 09 November 2022

CITATION
Liu H, Zhang Z, Du H and Cong T (2022), Numerical study on the heat transfer characteristics of a liquid lead–bismuth eutectic in a D-type channel. *Front. Energy Res.* 10:1041900. doi: 10.3389/fenrg.2022.1041900

Numerical study on the heat transfer characteristics of a liquid lead–bismuth eutectic in a D-type channel

Hong Liu[1], Zhigang Zhang[1]*, Haisu Du[1] and Tenglong Cong[2]

[1]Fundamental Science on Nuclear Safety and Simulation Technology Laboratory, Harbin Engineering University, Harbin, China, [2]School of Mechanical Engineering, Shanghai Jiao Tong University, Shanghai, China

A printed circuit heat exchanger (PCHE) can offer superior performance in area concentration and heat transfer efficiency. A PCHE with a liquid lead–bismuth eutectic (LBE) and supercritical carbon dioxide as working media can use these materials as intermediate heat exchangers in lead–bismuth eutectic-cooled reactors to reduce facility size and improve economy. To ensure the reliability of a numerical simulation for a liquid LBE in PCHE channels, the flow and heat transfer characteristics of a liquid LBE were investigated in a single D-type channel. The existing turbulent Prandtl number (Pr_t) models and the shear–stress transport (SST) $k-\omega$ model were evaluated first by using experimental liquid metal data. Then, a suitable Pr_t model was proposed for the numerical simulation of the liquid LBE. Finally, the flow and heat transfer characteristics of the liquid LBE were studied in D-type straight channels and D-type zigzag channels. The study presented the effects of flow velocity, wall heat flux, equivalent diameter and zigzag channel angle on the flow resistance and heat transfer characteristics. Meanwhile, a heat transfer correlation suitable for a D-type straight channel was also proposed. The research results in this paper lay a good foundation for the development of PCHEs with an LBE as the working fluid.

KEYWORDS

printed circuit heat exchange, turbulent Prandtl number, lead-bismuth eutectic, D-type channel, heat transfer correlation

1 Introduction

Liquid–metal cooled nuclear reactors are recognized as promising generation-IV reactors due to their low melting point, high boiling point, excellent heat absorption capacity, high molecular heat conduction, good neutron performance and radiation resistance. Moreover, the liquid lead alloy (typically a liquid lead–bismuth eutectic) offers good passive safety characteristics and superior economy as a coolant for nuclear reactors (Roelofs et al., 2019). The main characteristics of typical lead-based fast reactors (LFRs) worldwide have been summarized by Zhang et al. (2020). They noted the current

challenges in their development and discussed the research progress of four main thermohydraulic aspects.

The flow and heat transfer characteristics of liquid lead–bismuth eutectics (LBEs) have been studied extensively by experiments and numerical simulations. An experiment considering a 19-pin hexagonal rod bundle cooled by a forced-convective LBE was completed at the Karlsruhe Liquid Metal Laboratory (KALLA) (Pacio et al., 2016). Their experimental results had good repeatability in the uncertainty range, and correlations for predicting the drag coefficient and Nusselt number (Nu) were recommended. Moreover, research on the flow and heat transfer characteristics of a liquid LBE in annular channels has been conducted. An experimental investigation in the annular channel showed that the flow and heat transfer characteristics of a liquid LBE are obviously influenced by gas injection (Zhu et al., 2019). To overcome these experimental limitations, numerical simulations have been widely applied in analysing heat transfer characteristics. The RANS method and turbulent viscosity model were used to predict the forced convective heat transfer of a liquid LBE (Thiele and Anglart, 2013). Turbulent heat fluxes were modelled with a simple gradient diffusion hypothesis (Marocco et al., 2017), and the results showed that the turbulent Prandtl number (Pr_t) can be locally evaluated either with a correlation or by solving some additional transport equations. Furthermore, mixed large eddy simulation (LES) and direct numerical simulation (DNS) methods were also used to calculate the mixed convection of a liquid metal (Marocco and Garita, 2018), and the difference between the forced and assisted convection for the liquid metal was assessed at the same Reynolds number in detail. In addition, the flow and heat transfer characteristics of a liquid LBE in circular pipes were extensively studied. The heat transfer characteristics of a liquid LBE were also studied by experiments and numerical simulations methods in circular pipes (Chen et al., 2013). First, the numerical simulation results of different Pr_t models were evaluated. Then, they recommended a Pr_t model suitable for a liquid LBE in their investigation. The standard $k-\varepsilon$ model was adopted to analyse the heat transfer and flow characteristics of a liquid LBE in circular tubes under different heat flux conditions (Guo and Huai, 2013). The research results showed that the heat transfer entropy generation rate decreased with increasing Peclet number (Pe), and the fluid friction entropy generation rate increased. The direct numerical simulation method was used to calculate the liquid LBE in a vertical heating tube (Zhao et al., 2018). The study showed that when the turbulence attenuation increases with increasing buoyancy, the surface friction coefficient decreases significantly, and Nu decreases slightly. The physical properties of 12 liquid metals were collected and analysed by Jaeger (2016), and the heat transfer correlations in circular tubes, rectangular channels and circular channels were evaluated and compared with the experimental data. Moreover, the influence of inlet on heat transfer characteristics was analysed (Jaeger 2017). Jaeger predicted that the heat transfer at the inlet is 100% higher than that at the fully developed fluid and emphasized that optimizing the heat exchanger structure is helpful when strengthening the heat transfer.

In a nuclear reactor, heat is transferred from the primary circuit to a secondary circuit through an intermediate heat exchanger, and a regenerator is arranged in the second loop. The intermediate heat exchanger and the regenerator take the form of a shell and tube heat exchanger. This configuration requires that both heat exchangers have high heat transfer efficiency, and the safety of the heat exchangers must be guaranteed. Usually, shell and tube heat exchangers are used in conventional nuclear power plants. In recent years, the application of gas Brayton cycle power generation systems in liquid metal reactors has attracted extensive attention. Therefore, the characteristics between liquid metals and gas have been investigated. A numerical simulation method was used to analyse the characteristics of heat transfer and flow resistance between a liquid LBE and helium (Chen et al., 2013). Wang et al. (2017) experimentally investigated the heat transfer characteristics of a liquid LBE and helium in a heat exchanger, and the influences of inlet temperature and inlet fluid mass flow rate on the total heat transfer coefficient were analysed. Liu et al. (2018) designed a noncontact double-wall straight tube heat exchanger for a Kylin-II circuit, and the SST $k-\omega$ model was adopted to calculate the flow rate and temperature distribution of a liquid LBE in the heat exchanger. However, shell and tube heat exchangers are traditional heat exchanger equipment and cannot offer superior performance in area concentration and heat transfer efficiency.

It is well known that the heat needed to be recovered in the gas Brayton cycle is considerable, so the heat exchange efficiency and size of the regenerator are more prominent (Xu et al., 2020). Compared with shell and tube heat exchangers, printed circuit heat exchangers (PCHEs) have been applied in thermal power and solar power generation systems because of their high heat exchange efficiency, small size and high safety. The development of supercritical carbon dioxide flow and heat transfer characteristics have been classified and summarized in PCHEs according to experimental and numerical simulation results (Huang et al., 2019). An experimental study was conducted on a PCHE regenerator with discontinuous biased rectangular and airfoil fins (Pidaparti et al., 2019), and the local and average heat transfer coefficients and pressure drops under different operating conditions related to the supercritical carbon dioxide (SCO_2)-Brayton cycle were measured. Li et al. (2019) studied the influence of inlet temperature and pressure of SCO_2 on the overall heat transfer performance of a sawtooth finned PCHE, and an evaluation method was proposed for the overall heat transfer performance considering the influence of operating temperature and pressure. Aneesh et al. (2018) performed a numerical analysis on a simplified numerical model of a single-

row PCHE in a helium–helium countercurrent loop and studied the properties of local flow and heat transfer in a periodic channel. Saeed and Kim, 2017 performed a regional optimization of a SCO_2 PCHE, which significantly reduced the computation time without affecting the accuracy of the solution.

Most of the literature above has shown PCHEs used as regenerators in the Breton cycle, and the heat transfer characteristics were mainly studied between gases. However, there are few studies on PCHEs as intermediate heat exchangers for primary and secondary circuits of nuclear reactors. The thermal-hydraulic performance of a PCHE was studied with FLiNaK and helium as working fluids (Kim and Sun. 2014), and a reasonable PCHE design method was proposed. FLiNaK and carbon dioxide as working fluids were considered in a PCHE by Kim et al. (2016). They evaluated the influences of the different channel types on economy and proposed the best kinds of channel configuration for PCHEs. To obtain the heat transfer characteristics of SCO_2 and liquid metal in PCHEs, Cong et al. (2021) performed a numerical simulation on liquid metal sodium and SCO_2 by using SST $k-\omega$ and Abid low Reynolds $k-\varepsilon$ turbulence models for SCO_2 and sodium domains, respectively. They compared the heat transfer coefficient and friction coefficient calculated by numerical simulation with the empirical correlation. It was concluded that the mass flow and inlet working medium temperature have a significant influence on the heat transfer of the two kinds of working fluids.

At present, model tests and numerical simulations of liquid LBEs are widely performed in circular pipes, annular channels or outside tube bundles. Meanwhile, the heat transfer characteristics of fluids in the D-type channels of PCHEs are mainly focused on fluids such as supercritical carbon dioxide, helium and sodium. Nevertheless, no experimental data or simulation results for the flow and heat transfer characteristics of a liquid LBE in D-type channels have been published thus far. In the current work, to predict the convective heat transfer characteristics of a liquid LBE, a numerical simulation method with the SST $k-\omega$ model was performed in a single D-type channel of a PCHE. A new Pr_t model was proposed that is suitable for the numerical simulation of a liquid LBE. Meanwhile, a new correlation for calculating the heat transfer of D-type channels was also proposed. These research results can be used for developing a liquid metal PCHE that can be applied to a generation-reactor.

2 Numerical calculation models and methods

2.1 Geometry of the D-type channel

A PCHE is fabricated by flat metal plates with photochemically etched D-type channels. The diameter of the D-type channel is generally 1–2 mm. Compared with shell and tube heat exchangers, the PCHE has a smaller size and superior heat transfer efficiency; the diffusion welding process is used to ensure safety. In this paper, the heat transfer and resistance characteristics of D-type channels with different equivalent diameters are studied by a numerical simulation method. Based on the operational experience of a Russian liquid lead–bismuth reactor, it is believed that the liquid flow rate should be less than 2 m/s because mechanical corrosion can become a serious problem when the fluid velocity is high, especially for liquid heavy metals (Zhang et al., 2013). Therefore, the flow and heat transfer characteristics of the liquid LBE were studied at velocities of 0.2–2.2 m/s in this paper. The structural details of the D-type channel are shown in Figure 1. A shows a straight channel model, B and C show zigzag channels with different angles, and D shows a cross section of the D-type channel. Numerical simulation working conditions and the structural details for the D-type channels are described in Table 1.

2.2 Governing equations for flow and heat transfer

In recent years, computational fluid dynamics (CFD) has been widely used in the prediction of flow and heat transfer characteristics of liquid metals. Under the condition of constant wall heat flux, the $k-\varepsilon$ model was used to evaluate Pr_t in a two-dimensional model by Cheng and Tak. (2006); they proposed Cheng's Pr_t model. The $k-\varepsilon$ model was also adopted to calculate the heat transfer of a liquid LBE in a three-dimensional circular pipe (Chen et al., 2013); they evaluated Pr_t models and suggested correlations of Nu and Pr_t. However, the near-the-wall function was used to estimate the heat transfer in the $k-\varepsilon$ model, which cannot accurately calculate the heat transfer of the fluid in the viscous sublayer. The real heat transfer of the fluid in the viscous sublayer is bound to affect the accuracy of the numerical simulation results. Therefore, it is necessary to reassess the Pr_t model of a liquid LBE in the near wall. Although direct numerical simulation (DNS) and large eddy simulation (LES) can well calculate the real flow and heat transfer of a fluid near a wall, they are not suitable for engineering projects due to the large grid quantity. The $k-\omega$ model can be used to calculate the flow and heat transfer characteristics of a fluid near a wall; however, the $k-\varepsilon$ model is used to calculate the flow and heat transfer characteristics of the fluid outside the boundary layer. Moreover, the computational resources required by the $k-\omega$ model are far less than those of the DNS and LES. The $k-\omega$ model is considered an advantageous computational model for future engineering applications.

To comprehensively assess the applicability of the Pr_t models and study the flow and heat transfer characteristics of a liquid LBE, the SST $k-\omega$ model was adopted. The SST $k-\omega$ model can not only accurately calculate the flow and heat transfer in the viscous sublayer but also avoid the sensitivity of the standard $k-\omega$ model to incoming flow (Menter. 1993). The solved governing equations are as follows:

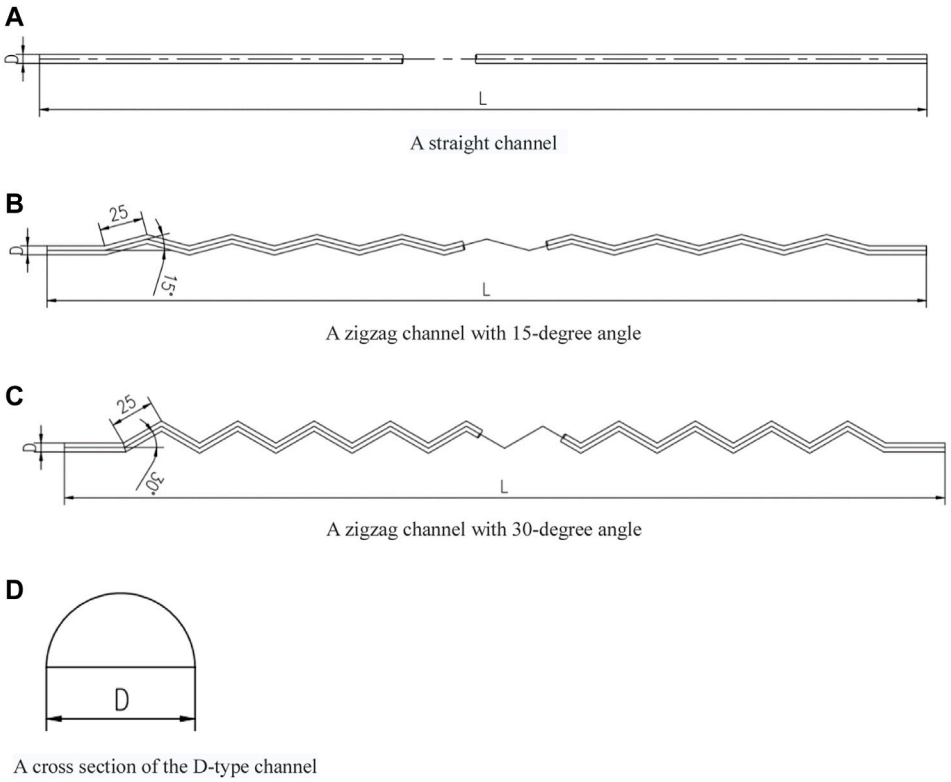

FIGURE 1
Geometry of the D-type channel.

TABLE 1 Numerical simulation working conditions for the D-type channels.

Case no.	D-type channel diameter(mm)	Equivalent diameter (mm)	Channel length (mm)	Velocity (m/s)	Wall heat flux (kW/m^2)	Inlet temperature (K)	Channel form
#1	10	6.11	900	0.2–2.2	−200	773.15	Straight channel
#2	7.5	4.58	900	0.2–2.2	−200	773.15	Straight channel
#3	5	3.05	900	0.2–2.2	−200	773.15	Straight channel
#4	2.5	1.53	900	0.2–2.2	−200	773.15	Straight channel
#5	10	6.11	900	0.2–2.2	−200	773.15	Straight channel
#6	5	6.11	900	1.0	−500 −100	773.15	Straight channel
#7	5	6.11	900	1.0	−200	573.15–773.15	Straight channel
#8	5	3.05	900	0.2–2.2	−200	773.15	zigzag channel(15°)
#9	5	3.05	900	0.2–2.2	−200	773.15	zigzag channel(30°)

TABLE 2 Constants used in the turbulence models.

$\sigma_{k,1}$	$\sigma_{\omega,1}$	$\sigma_{k,2}$	$\sigma_{\omega,2}$	α_1	$\beta_{i,1}$	$\beta_{i,2}$
1.176	2.0	1.0	1.168	0.31	0.075	0.0828

Mass equation:

$$\frac{\partial \rho}{\partial t} + \frac{\partial}{\partial x_i}(\rho u_i) = 0 \tag{1}$$

Momentum equation:

$$\frac{\partial}{\partial t}(\rho \overline{u_i}) + \frac{\partial}{\partial x_j}(\rho u_i u_j) = -\frac{\partial p}{\partial x_i} + \frac{\partial}{\partial x_j}(\sigma_{ij}) + \frac{\partial}{\partial x_j}\left(\mu_t\left(\frac{\partial u_i}{\partial x_j} + \frac{\partial u_j}{\partial x_i}\right) - \frac{2}{3}\left(\rho k + \mu_t \frac{\partial u_k}{\partial x_k}\right)\delta_{ij}\right) \tag{2}$$

Energy equation:

$$\frac{\partial}{\partial t}(\rho E) + \frac{\partial}{\partial x_i}(u_i(\rho E + p)) = \frac{\partial}{\partial x_j}\left(\left(k + \frac{c_p \mu_t}{Pr_t}\right)\frac{\partial T}{\partial x_j} + u_i(\tau_{ij})_{eff}\right) + S_h \tag{3}$$

where $\rho, u, p, \mu, \mu_t, k, T, c_p, (\tau_{ij})_{eff}, E, S_h, \sigma_{ij}$, and Pr_t are the density, velocity, pressure, laminar viscosity, turbulent viscosity, thermal conductivity, temperature, specific heat, deviatoric stress tensor, total energy, source items, stress tensor, and turbulent Prandtl number, respectively.

Shear–stress transport (SST) k–ω equations:

$$\frac{\partial}{\partial t}(\rho k) + \frac{\partial}{\partial x_i}(\rho k u_i) = \frac{\partial}{\partial x_j}\left[(\mu + \frac{\mu_t}{\sigma_k})\frac{\partial k}{\partial x_j}\right] + G_k - Y_k + S_k \tag{4}$$

$$\frac{\partial}{\partial t}(\rho \omega) + \frac{\partial}{\partial x_i}(\rho \omega u_i) = \frac{\partial}{\partial x_j}\left[(\mu + \frac{\mu_t}{\sigma_\omega})\frac{\partial \omega}{\partial x_j}\right] + G_\omega - Y_\omega + S_\omega \tag{5}$$

where G_k represents the production rate of turbulence due to the mean velocity gradients, G_ω represents the production ω, Y_k represents the dissipation of k due to turbulence, Y_ω represents the dissipation of ω due to turbulence, and S_k and S_ω represent source items for the user. σ_k represents the turbulent Prandtl number for turbulent kinetic energy k, and σ_ω represents the turbulent Prandtl number of specific dissipation rate ω.

$$\mu_t = \alpha^* \frac{\rho k}{\omega} \tag{6}$$

where α^* can reduce the viscosity of turbulence to correct for low Reynolds number

$$\alpha^* = \alpha^*_\infty \left(\frac{\alpha^*_0 + Re_t/R_k}{1 + Re_t/R_k}\right) \tag{7}$$

where $e_t = \frac{\rho k}{\mu \omega}$, $R_k = 6$, $\alpha^*_0 = \frac{\beta_i}{3}$, and $\beta_i = 0.072$.

At a high Reynolds number, $\alpha^* = \alpha^*_\infty = 1$. To accurately calculate the influence of the turbulent Prandtl number (Pr_t) on heat transfer characteristics at low Reynolds numbers, turbulent shear stress should be considered in the definition of turbulent viscosity in the SST $k-\omega$ model. The calculation method of μ_t is given in Eq. 8. This model is more accurate and reliable than the standard $k-\omega$ model and has a wider application range.

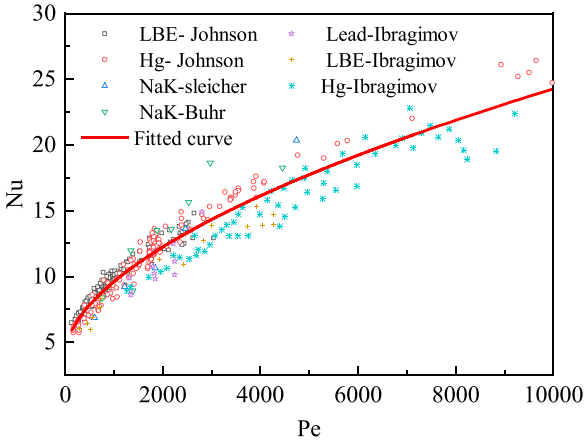

FIGURE 2
Experimental data and the fitted curve.

Turbulent viscosity:

$$\mu_t = \frac{\rho k}{\omega} \frac{1}{\max\left[\frac{1}{\alpha^*}, \frac{SF_2}{\alpha_1 \omega}\right]} \tag{8}$$

$$F_2 = \tanh(\phi_2^2) \tag{9}$$

$$\phi_2 = \max\left[2\frac{\sqrt{k}}{0.09\omega y}, \frac{500\mu}{\rho y^2 \omega}\right] \tag{10}$$

where y is the distance to the next surface.

The constants in the SST $k-\omega$ turbulence model are presented in Table 2. More details on the SST $k-\omega$ model can be found in Menter (1994).

3 Assessment of heat transfer correlations and Pr_t models

3.1 Assessment of heat transfer correlations

For liquid metals, numerous correlations have been proposed for convective heat transfer calculations by theoretical analysis and experimental research. Universally, the Nusselt number (Nu) is expressed as a function of the Prandtl number (Pr) and Peclet number (Pe). The correlation of heat transfer is given in the following.

$$Nu = a + bPr^m Pe^n \tag{11}$$

TABLE 3 Convective heat transfer correlation for liquid metals.

Investigator	Correlation	Remark
Lyon (1951)	$Nu = 7.0 + 0.025(Pe/Pr_t)^{0.8}$	$0 < Pr < 0.1$
		$4 \times 10^4 < Re < 3.24 \times 10^6$
Skupinski et al. (1965)	$Nu = 4.82 + 0.0185Pe^{0.827}$	$10^4 < Re < 5 \times 10^6$
Kirillov et al. (2001)	$Nu = 4.5 + 0.018Pe^{0.8}$	$10^4 < Re < 5 \times 10^6$
Azer and Chao. (1961)	$Nu = 7.0 + 0.05Pr^{0.25}Pe^{0.77}$	$0 < Pr < 0.1$
		$0 < Pe < 1.5 \times 10^4$
Sleicher et al. (1973)	$Nu = 6.3 + 0.0167Pr^{0.08}Pe^{0.85}$	$0.004 < Pr < 0.1$
		$10^4 < Re < 10^6$
Chen and Chiou. (1981)	$Nu = 5.6 + 0.0165Pr^{0.01}Pe^{0.85}$	$0 < Pr < 0.1$
		$10^4 < Re < 5 \times 10^6$
Stromquist (1953)	$Nu = 3.6 + 0.018Pe^{0.8}$	$88 < Pe < 4000$
Subbotin et al. (1963)	$Nu = 5 + 0.025Pe^{0.8}$	
Ibragimov et al. (1962)	$Nu = 4.5 + 0.014Pe^{0.8}$	
Cheng and Tak. (2006)	$Nu = A + 0.018Pe^{0.8}$	$A = \begin{cases} 4.5 & Pe \le 1000 \\ 5.4 - 9 \times 10^{-4}\,Pe & 1000 \le Pe \le 2000 \\ 3.6 & Pe \ge 2000 \end{cases}$

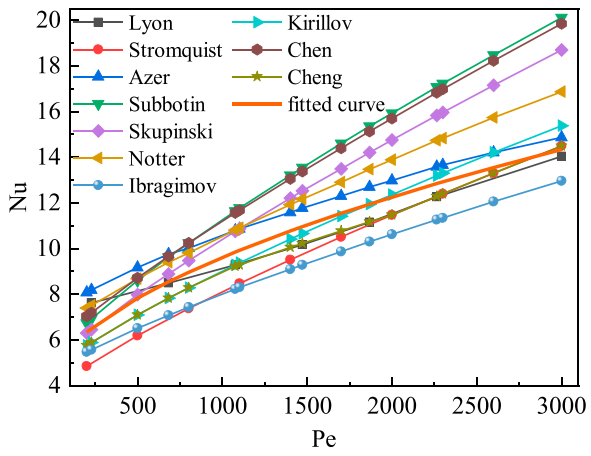

FIGURE 3
Comparison of heat transfer correlations and the fitted curve in Figure 2.

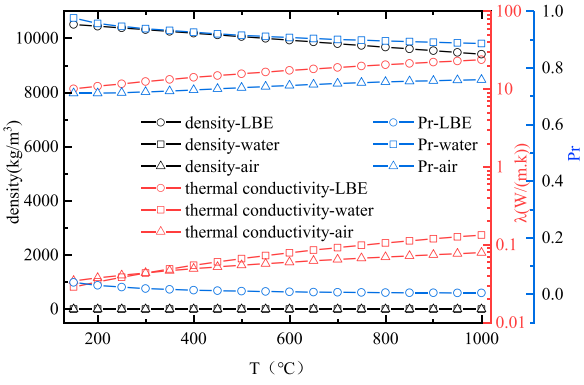

FIGURE 4
Variation in the physical properties of liquid LBE, air and water with different temperatures.

where α, b, m, and n are all constants.

Johnson et al. (1953), Buhr et al. (1968) and Ibragimov et al. (1962) used experimental methods to investigate the heat transfer characteristics of a liquid LBE in a vertical circular pipe, and they obtained experimental data in the range of 200–10,000. The experimental data and their fitted curves are presented in Figure 2. The correlations proposed by scholars are summarized in Table 3; a comparison between the fitted curves of the experimental data and the correlations proposed by scholars is shown in Figure 3.

As seen in Figure 2, the calculation results of the correlations proposed by Lyon. (1951), Stromquist (1953), Azer and Chao. (1961), Skupinski et al. (1965), Chen and Chiou. (1981), Sleicher et al. (1973) and Subbotin et al. (1963) are larger than the fitted curve, and the deviations are large. The calculated result of the correlation proposed by Ibragimov et al. (1962) is less than the fitted curve. Therefore, these models are not effective in describing the turbulent heat transfer of liquid metals. The heat transfer correlation proposed by Cheng and Tak. (2006) is in piecewise form. When Pe is less than 1,000, the correlation proposed by Kirillov et al. (2001) is adopted. When Pe is more than 2000, Stromquist's correlation is recommended. When $1000 < Pe < 3000$, a new correlation was reproposed. The

TABLE 4 Turbulent Prandtl number models of liquid metals.

Investigator	Correlation	Remark
Aoki. (1963)	$Pr_t^{-1} = 0.014Re^{0.45}Pr^{0.2}[1 - \exp(-1/0.014Re^{0.45}Pr^{0.2})]$	
Reynolds (1975)	$Pr_t = (1 + 100Pe^{-0.5})(1/1 + 120Re^{-0.5} - 0.15)$	
Jischa and Rieke. (1979)	$Pr_t = 0.9 + \frac{182.4}{PrRe^{0.888}}$	
Kays. (1994)	$Pr_t = 0.85 + 0.7/Pe_t$	
Chen et al. (2013)	$Pr_t = \begin{cases} 4.12 & Pe \le 1000 \\ 0.01Pe/[0.018Pe^{0.8} - (7.0 - A)]^{1.25} & 1000 \le Pe \le 6000 \end{cases}$	$A = \begin{cases} 5.4 - 9 \times 10^{-4}Pe & 1000 \le Pe \le 2000 \\ 3.6 & 2000 \le Pe \le 6000 \end{cases}$
ANSYS Default value	$Pr_t = 0.85$	

maximum deviation between Cheng's model and the fitted curve is less than 13.5%. Figure 3 shows that the correlations proposed by Kirillov agree well with the calculated results of the fitted curve, and the maximum deviation is less than 10%. Through comparative analysis, it is recommended to use the correlation proposed by Kirillov to assess the Pr_t model for a liquid LBE under the condition of constant wall heat flux.

3.2 Assessment of Pr_t models

The melting point of the liquid LBE is 125°C, and the physical properties of the liquid LBE are only a function of temperature (Organisation For Economic Co-Operation And Development Nuclear Energy Agency, 2015). At atmospheric pressure, the physical parameters of the liquid LBE are completely different from those of conventional fluids such as air and water. The density of the liquid LBE is 12,500–35,000 times that of air and 20,000–55,000 times that of water in the range of 150–1,000°C. The Prandtl number (Pr) of the liquid LBE is 6.5‰–6.5% for air and 5‰–4.3% for water. The thermal conductivity of the liquid LBE is 285–300 times that of air and 170–350 times that of water. The variation trends of the liquid LBE, air and water vapour with temperature are shown in Figure 4. The Pr of the liquid LBE is much smaller than that of a conventional fluid, but its thermal conductivity is three orders of magnitude higher than that of a conventional fluid. As a result, the fluid molecular thermal conductivity still dominates, even in a turbulent flow state. Therefore, the Pr_t model applied to a conventional fluid is no longer suitable for a liquid LBE.

3.2.1 Turbulent Prandtl number model

For conventional fluids, Pr is defined as the ratio of kinematic viscosity to thermal diffusivity, which reflects the comparison between momentum diffusion and thermal diffusivity. Similar to the molecular Prandtl number, Pr_t is defined as the ratio of momentum vortex diffusivity to heat transfer vortex diffusivity. The correlation of Pr_t is calculated according to Eq. 12 (Kays et al., 2004). To accurately calculate

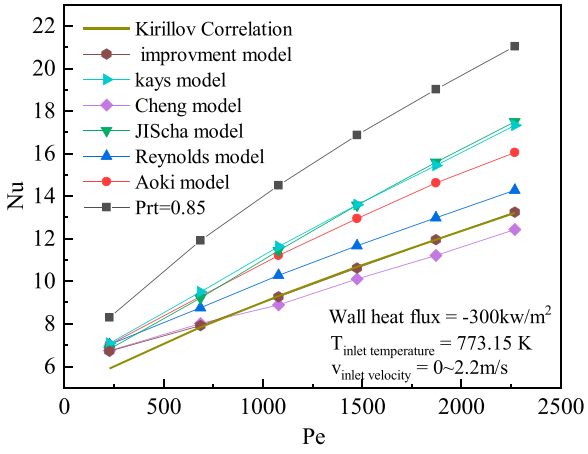

FIGURE 5
Comparison between the calculation results of 7 Pr_t models and Kirillov's correlation.

Pr_t, data such as the gradient of the mean temperature and velocity, turbulent shear stress and turbulent heat flux should be measured. In general, turbulent heat transport is strictly analogous to turbulent momentum transport (Groetzbach. 2003).

$$Pr_t = \frac{\varepsilon_M}{\varepsilon_H} = \frac{\overline{u_x' u_y'} \frac{\partial \overline{T}}{\partial y}}{\overline{T' u_y'} \frac{\partial u_x}{\partial y}} \tag{12}$$

where ε_M represents momentum vortex diffusivity, ε_H represents heat transfer vortex diffusivity, and $\overline{u_x'}$, $\overline{u_y'}$, and $\overline{T'}$ are the average velocity and temperature.

To obtain more accurate prediction results, the SST $k-\omega$ model is used to assess the Pr_t models, which are summarized in Table 4, including the constant model with $Pr_t = 0.85$.

The Pr_t models proposed by Cheng, Aoki, Reynolds and Jischa are a series of global parameters related to flowing/transport conditions, such as Pr, Re (or Pe), which are equivalent to a fixed value on a certain cross section and do not involve the local spatial distribution of parameters. The

TABLE 5 Geometry and numerical calculation boundary conditions.

Name	Units	Value
Diameter	mm	5, 10, 15, 20, 25
Length	mm	1,500–2,500
Inlet temperature	°C	500
Wall heat flux	kw/m^2	−500 −100
Inlet velocity	m/s	0.2–2.2

TABLE 6 Grid independence verification.

Case no.	Grid number	Nu	Pressure drops (Pa)
1	346,500	12.67	13,499
2	478,500	12.83	13,868
3	630,500	12.88	14,087
4	770,000	13.0	14,342
5	927,500	13.03	14,403

Pr_t model proposed by Kays is a function of the turbulent Pe number, as shown in Table 4. The turbulent Pe number is a function of the turbulent viscosity ratio and Pr, which is shown in Eq. 13. The turbulent viscosity ratio is a local spatial parameter that needs to be extracted and updated in each simulation iteration during the numerical calculation. Duponcheel et al. (2014) verified that the Kays model was the best choice, which was in good agreement with LES results, but there is still a large discrepancy between the experimental data and the calculated results using the $k-\omega$ model. To improve the prediction accuracy of the heat transfer of the liquid metal, the Kays model was modified, and the constant 0.7 was replaced by 3.5 in the Kays model, the improved model was then proposed as shown in Eq. 14. The numerical simulation result of Nu calculated by Eq. 14 agrees with the correlation best, and the numerical results comparison of each Pr_t model can be found in Figure 5. The Eq. 14 can be applied to liquid metal sodium, lead-bismuth eutectic, sodium-potassium alloy and mercury.

$$Pe_t = \frac{\mu_t}{\mu} p_r \tag{13}$$

$$Pr_t = 0.85 + \frac{3.5}{Pe_t} \tag{14}$$

3.2.2 Assessment of the Pr_t model

3.2.2.1 Mesh independency verification

The physical properties of the liquid LBE, such as viscosity, specific heat, thermal conductivity and density, are based on the thermophysical relationships recommended in the guidance manual prepared by the Organization for Economic Cooperation and Development and Nuclear Energy Agency (OECD/NEA) (Organisation For Economic Co-Operation And Development Nuclear Energy Agency, 2015). In this paper, the Pr_t models of the liquid LBE were evaluated in a vertical circular pipe. The geometry of the circular pipe and the calculation boundary conditions are described in Table 5.

The structured mesh with O-type division is adopted for the calculation model, and the grid quantity of meshes ranges between 346,500 and 957,500. The number of boundary layers is set to 10, y+<1, and the Pr_t number is assumed to be 0.85. Without considering the influence of gravity, the pressure drops and Nu of liquid LBE with different grid quantities are obtained by numerical simulation. The calculation results are shown in Table 6.

The calculation results show that with the increase in the grid quantity, the difference in liquid LBE pressure drops and Nu decreases. The Nu deviations between the grid quantity of 630,500 and 770,000, 770,000 and 927,500 are less than 1%, and the pressure drop deviations are less than 1.7%, which indicates that the three grids are independent. Considering both the accuracy and the speed of the numerical simulation, the model with a grid quantity of 770,000 was selected to calculate the flow and heat transfer characteristics of the liquid LBE in a circular pipe.

3.2.2.2 Assessment of Pr_t models

In the present study, 7 Pr_t models were assessed by a numerical simulation method. The comparison between the calculation results and the correlation proposed by Kirillov is shown in Figure 5. The Pe number varies from 200 to 2,500. Under the same conditions of constant wall heat flux and inlet temperature conditions, numerical results show that Nu increases with increasing fluid velocity and Pe number. When Pe is larger than 500, the Nu calculated by the improvement model is in good agreement with the correlation proposed by Kirillov. When the Pe number is less than 500, the deviation with Kirillov's correlation is less than 10%, and as the PE number decreases, the calculation results of each Pr_t model have little difference.

To further verify the applicability of the Pr_t models at constant heat flux conditions, the numerical simulation was performed considering the changes in fluid temperature, wall heat flux, pipe tilt angle, and pipe diameter. As seen in Figure 6A, the results show that Nu increases with increasing wall heat flux when the fluid velocity and inlet temperature are constant, and the deviation between Nu calculated by numerical simulation and Kirillov's correlation is less than 1.4%. Figure 6B shows that Nu decreases with increasing inlet temperature when the wall heat flux and fluid velocity are constant, and the maximum deviation between Nu calculated by numerical simulation and

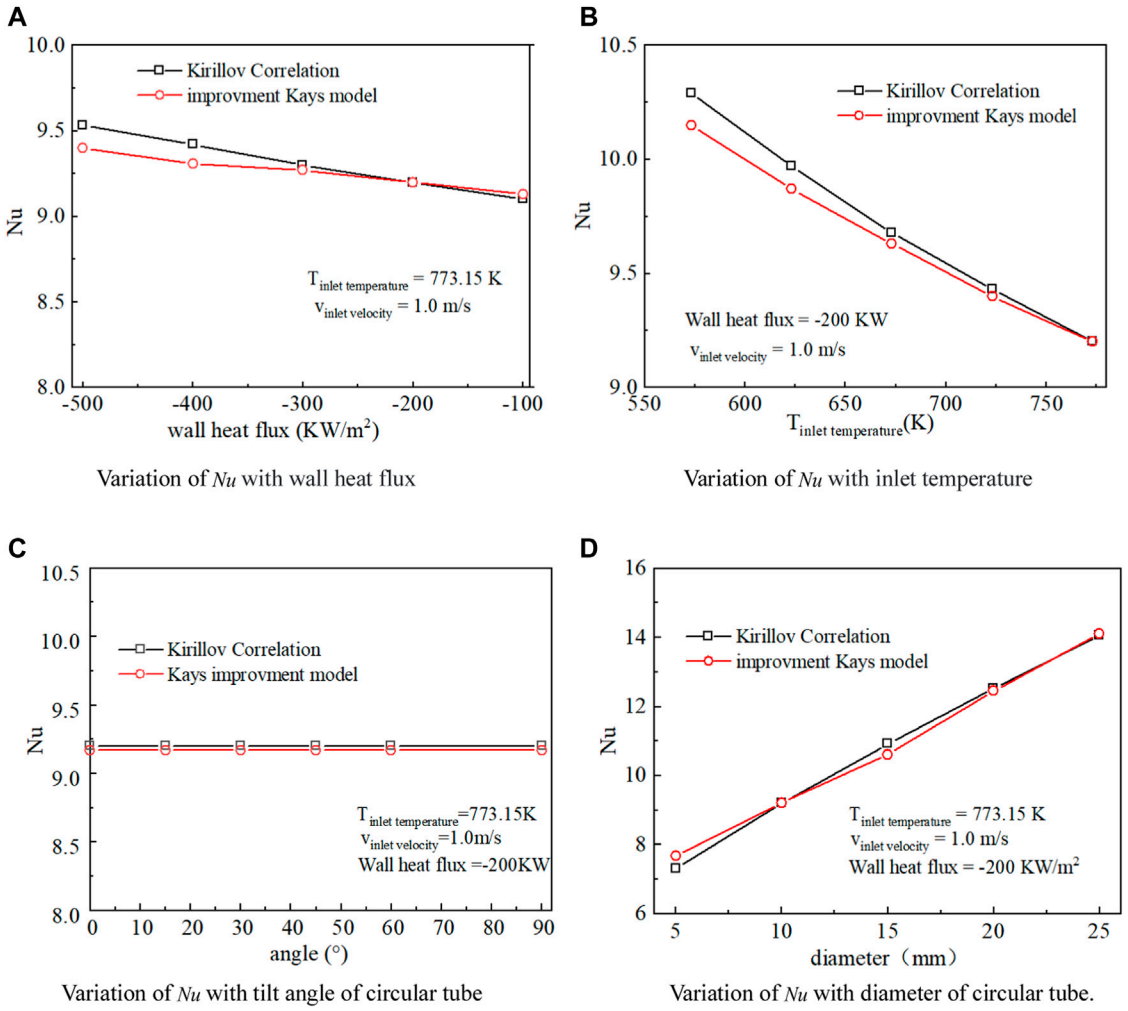

FIGURE 6
Variation of *Nu* with wall heat flux, inlet temperature, tilt angle and diameter.

Kirillov's correlation is less than 1.3%. Figure 6C illustrates that *Nu* basically did not change with increasing tube tilt angle when the wall temperature, fluid velocity and inlet temperature were constant, and the deviation between *Nu* calculated by numerical simulation and Kirillov's correlation was less than 0.3%. Figure 6D shows that *Nu* increases with increasing pipe diameter when the inlet fluid temperature, wall heat flux and fluid velocity are constant, and the deviation between *Nu* calculated by numerical simulation and Kirillov's correlation is less than 4.7%. The research results show that when the inlet temperature, wall heat flux, fluid velocity, tilt angle and pipe diameter change under the condition of constant wall heat flux, *Nu* calculated by the improvement model agrees well with the correlation proposed by Kirillov. The applicability of numerical methods and model have been verified with experimental data in circular channel. The Configuration of D-type channel is different from Circular

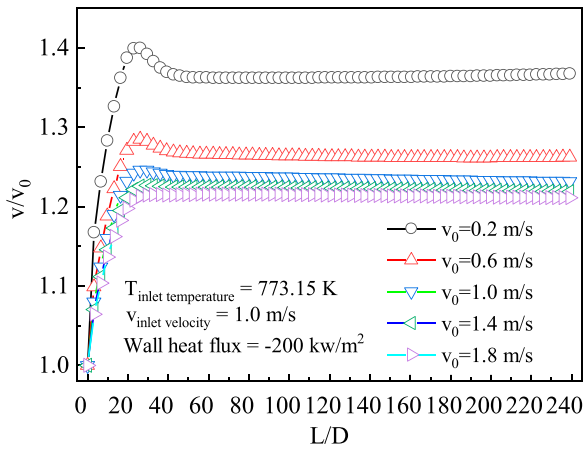

FIGURE 7
Variation in the velocity ratio along the circular tube.

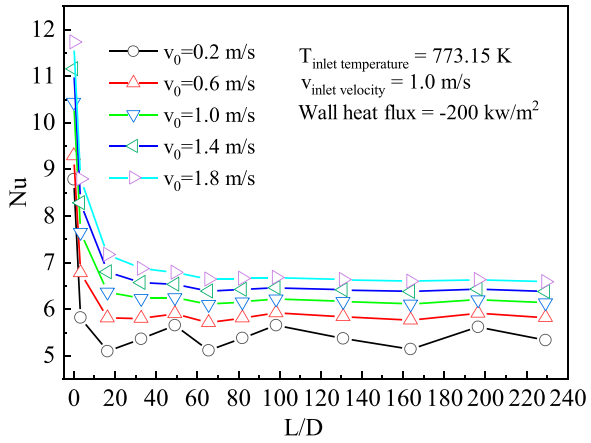

FIGURE 8
Variation of *Nu* along the circular tube.

channel. In this paper, the improvement Pr_t model was used to calculate the flow and heat transfer characteristics of the liquid LBE in the D-type channel.

4 Results and discussion

4.1 Variation in the velocity and heat transfer characteristics of a D-type straight channel

Taking a D-type straight channel with an equivalent diameter of 3.05 mm as an example, when the fluid velocity varies from 0.2 to 2.2 m/s and the inlet temperature of the liquid LBE and the wall heat flux are constants, the calculated results of the flow and heat transfer characteristics are analysed. Figure 7 shows that the centre flow velocity of the D-type channel reaches the maximum when L/D is

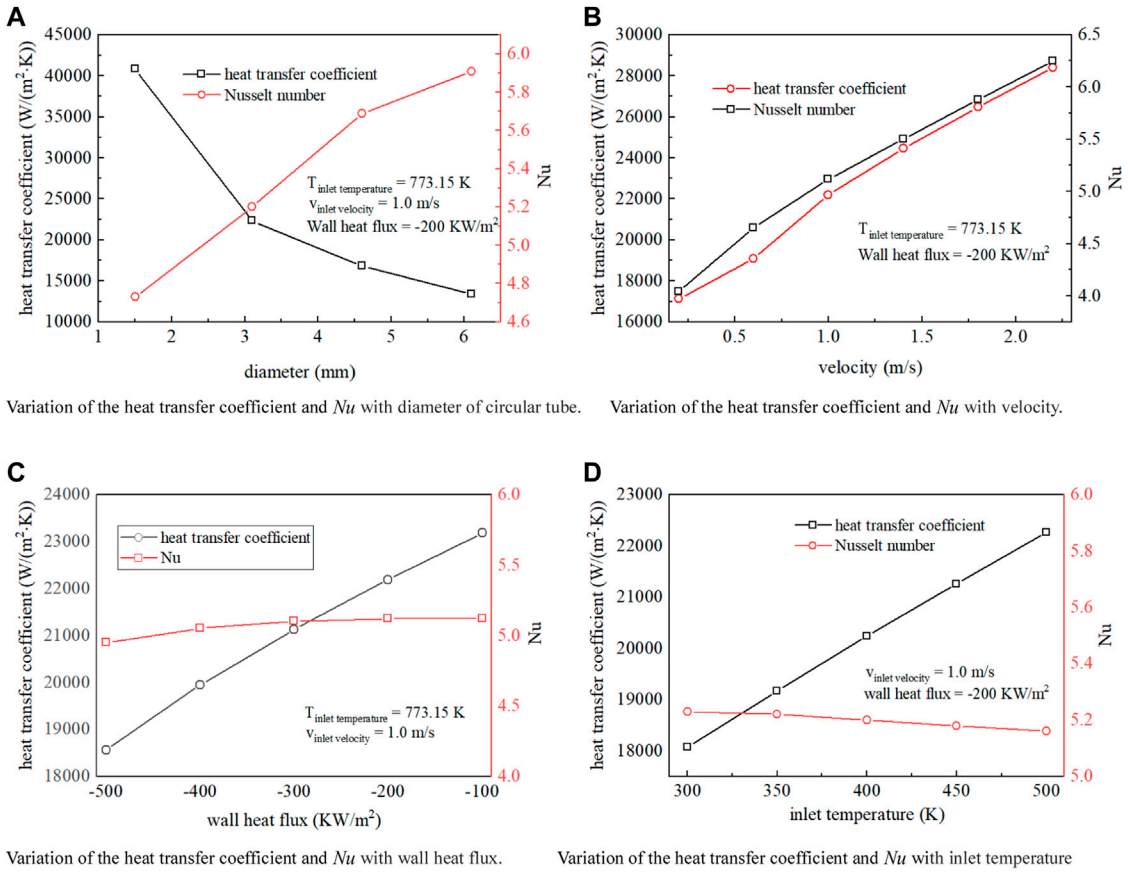

Variation of the heat transfer coefficient and *Nu* with diameter of circular tube.

Variation of the heat transfer coefficient and *Nu* with velocity.

Variation of the heat transfer coefficient and *Nu* with wall heat flux.

Variation of the heat transfer coefficient and *Nu* with inlet temperature

FIGURE 9
Variation of the heat transfer coefficient and *Nu* with diameter, velocity, wall heat flux and inlet temperature.

equal to 30. If the inlet fluid velocity is less than 1.0 m/s, the flow velocity decreases rapidly. When L/D is equal to 40, the flow velocity reaches a stable value, indicating that the liquid LBE has fully developed. When the fluid velocity is greater than 1.0 m/s, the fluid velocity reaches the maximum value and then maintains the stable value directly. Figure 8 illustrates that if the fluid velocity is low, the thickness of the boundary layer in the channel is large, and the heat transfer coefficient of the fluid fluctuates along the pipe length. When the flow velocity is greater than 1.0 m/s, the heat transfer coefficient of the fluid along the pipe length decreases to a certain value and then tends to be stable.

4.2 Analysis of the heat transfer characteristics of liquid LBE in straight channels

The liquid LBE in D-type channels with equivalent diameters of 1.53 mm, 3.05 mm, 4.58 mm and 6.1 mm were studied by a numerical simulation method, and the effects of diameters, fluid velocity, inlet temperature and wall heat flux on the heat transfer characteristics were analysed. As seen in Figure 9A, the calculation results show that *Nu* decreases gradually with decreasing diameter of the D-type channel at the given boundary conditions; however, the convective heat transfer coefficient increases gradually. This indicates that the microchannel heat exchanger has the advantage of a strong heat transfer capacity. The model with an equivalent diameter of 3.05 mm was adopted to analyse the effects of thermophysical properties on liquid LBE. Figure 9B illustrates the effect of the velocity on the heat transfer characteristics. The heat transfer coefficient and *Nu* of liquid LBE increase with increasing flow velocity. With the increase in flow velocity, the turbulent characteristics of the liquid LBE will be enhanced, which can effectively further strengthen the convective heat transfer characteristics of liquid LBE. Figure 9C shows that with the absolute value increase of the wall heat flux, the heat transfer coefficient of liquid LBE decreases greatly; however, *Nu* decreases slightly. When the absolute value of the wall heat flux increases, the temperature difference between the fluid and the wall gradually increases, so *Nu* only changes slightly. As shown in Figure 9D, the convective heat transfer coefficient of liquid LBE gradually increases with increasing fluid inlet temperature, but *Nu* slightly decreases. This indicates that if the fluid inlet temperature increases, the temperature difference between the fluid and wall gradually decreases, and the convective heat transfer characteristics of liquid lead–bismuth are strengthened.

Compared with the circular tube, for the special structural form of the D-type channel, under the condition of constant wall heat flux, the liquid LBE convective heat transfer correlation was proposed. The equation shown in Eq. 17. The application scope of *Pe* is from 100 to 1,500, the application scope of *Re* is from 8,000 to 130,000, the application scope of temperature is from 200°C to 550°C, and the fitting variance is 0.956.

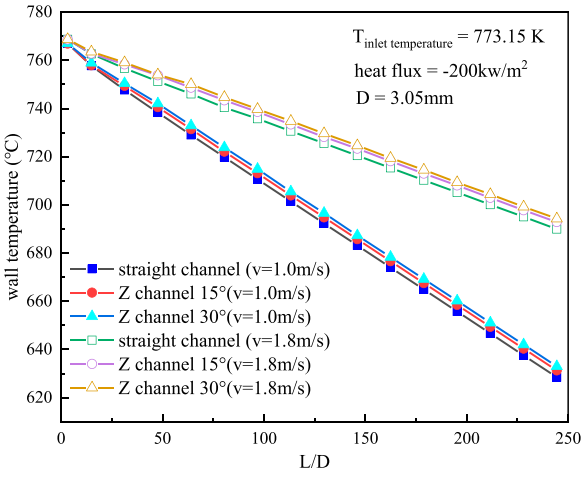

FIGURE 10
Variation in wall temperature along the circular tube for different D-type channels at different velocities.

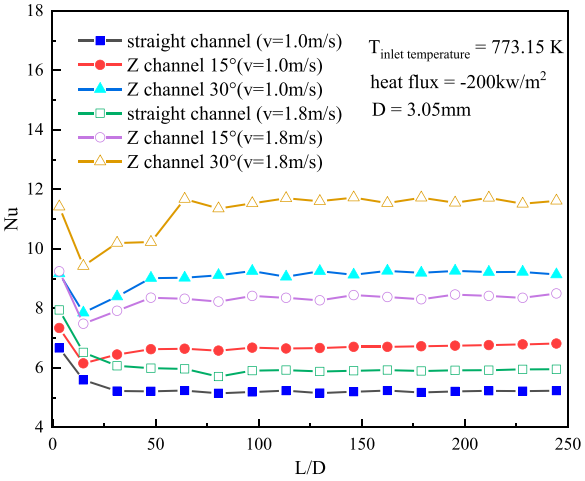

FIGURE 11
Variation in *Nu* along the circular tube for different D-type channels at different velocities.

$$Nu = 3.85 + 0.01Pe^{0.834} \quad (17)$$

4.3 Analysis of the heat transfer characteristics of liquid LBE in the zigzag channel

Generally, the design of a special structure can strengthen the heat transfer characteristics of the fluid. Numerical simulation calculation for the heat transfer characteristics

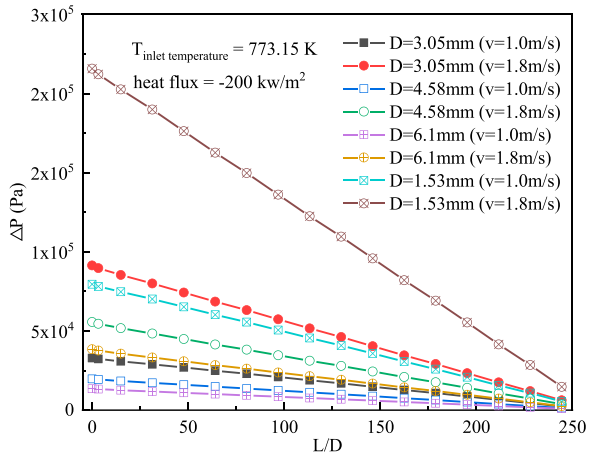

FIGURE 12
Variation in the pressure drop along the circular tube for different diameter channels at different velocities.

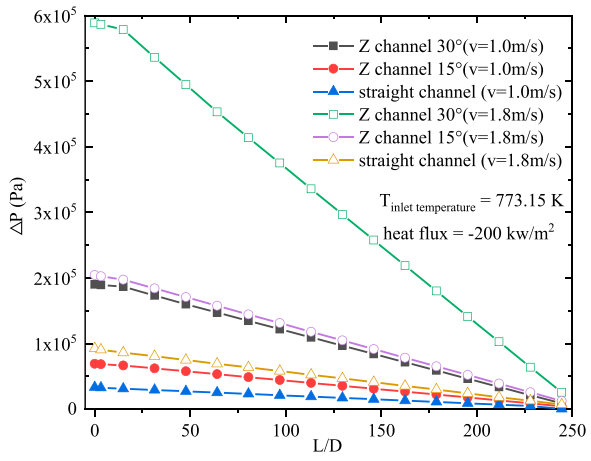

FIGURE 13
Variation in the pressure drop along the circular tube for different D-type channels at different velocities.

of liquid LBE was performed on the straight channel and the zigzag channel at the same boundary conditions. As seen in Figure 10, the wall temperature of the zigzag channel is higher than that of the straight channel at the same flow velocity. The calculation results also show that the wall temperature decreases with increasing flow velocity, and the wall temperature increases with increasing zigzag channel angle. As shown in Figure 11, with increasing fluid flow velocity, *Nu* increases. The *Nu* of liquid LBE in the Z-channel channel is higher than that in the straight channel at the same flow velocity, and the larger the angle of the Z-channel is, the larger the *Nu* of liquid LBE is. According to the analysis of the calculation results, the zigzag channel structure can strengthen the convective heat transfer characteristics of liquid LBE. Therefore, when the flow velocity of liquid LBE meets the requirement, the zigzag channel will be considered to enhance the convective heat transfer, which can effectively reduce the volume of the heat transfer equipment.

4.4 Analysis of the resistance characteristics of D-type channels

Although the design of the special structure can strengthen the convective heat transfer of the liquid LBE, it also increases the resistance of the fluid. In the current research, numerical simulation calculations were performed on the resistance characteristics of a straight channel with four equivalent diameters. As seen in Figure 12, at specified boundary conditions, the fluid resistance of liquid LBE increases with the velocity. At the same flow velocity, the smaller the equivalent diameter is, the greater the fluid resistance is. Figure 13 shows the resistance characteristics of the straight channel and zigzag channel. When the equivalent diameter of D-type channels and flow velocity are the same, the resistance of the fluid in the zigzag channel is greater than that in the straight channel, and the larger the angle of the zigzag channel is, the greater the resistance of the liquid LBE is, which is more obvious at high flow velocity. At the same zigzag channel angle, the fluid resistance increases with the flow velocity, which is in accord with the variation tendency of fluid resistance in the straight D-type channel, and the increase in fluid resistance is much larger than that caused by the increase in flow velocity in the straight channel. Therefore, if the design of the D-type channel heat exchanger is performed, the flow velocity of the fluid could not be too high, such as the choice of zigzag channel. It is suggested that the angle of the zigzag channel should not exceed 15°; otherwise, the resistance of the heat exchanger will be very large, resulting in the economic decline of the whole heat exchange system.

5 Conclusion

In this paper, the SST $k-\omega$ model was used to investigate the flow and heat transfer characteristics of liquid LBE in D-type channels. The main conclusions obtained from the present work are as follows:

1) The *Nu* calculated by the correlation proposed by Kirillov agrees well with the fitted curve of the experimental data

in a circular pipe at constant wall heat flux conditions, and the correlation proposed by Kirillov was used to assess the different Pr_t models in this paper.

2) To obtain the numerical simulation results of liquid LBE in a circular pipe, the improvement model was proposed in this paper. In addition, the improvement Pr_t model was used to calculate the heat transfer of liquid LBE at different boundary conditions, such as different fluid velocities, inlet temperatures, wall temperatures, fluid velocities, tube diameters and tube tilt angles. The numerical simulation results agree well with the heat transfer correlation proposed by Kirillov.
3) The heat transfer characteristics of liquid LBE were analysed in the current study, including variation of the heat transfer coefficient and Nu with equivalent diameter, wall heat flux, inlet fluid temperature and fluid velocity. A new correlation for calculating Nu of liquid LBE in the D-type straight channel was proposed.
4) The numerical simulation results of liquid LBE in D-type channels show that the heat transfer can be enhanced by reducing the equivalent of the D-channel or adopting a zigzag channel. The zigzag channel could obviously strengthen the heat transfer effect, but the increase in resistance was also particularly prominent. Therefore, it is necessary to comprehensively evaluate the resistance and heat transfer characteristics of zigzag channels when designing PCHEs with special D-type channels.

Data availability statement

The original contributions presented in the study are included in the article/Supplementary Material, further inquiries can be directed to the corresponding author.

Author contributions

HL: experimental data analysis, writing. ZZ: supervision, review and editing. HD: resources, conceptualization. TC: project review.

Funding

This research was supported by National Key R&D Program of China (grant number 2020YFB1901804), CNNC's Pilot-innovation Research Project, National Natural Science Foundation of China (grant number 52176151) and Fundamental Research Funds for the Central Universities of China (grant number 3072022TS1503).

Acknowledgments

The authors thank them for their financial support.

Conflict of interest

The authors declare that the research was conducted in the absence of any commercial or financial relationships that could be construed as a potential conflict of interest.

Publisher's note

References

Aneesh, A. M., Sharma, A., Srivastava, A., and Chaudhury, P. (2018). Effects of wavy channel configurations on thermal-hydraulic characteristics of printed circuit heat exchanger (pche). *Int. J. Heat Mass Transf.* 118, 304–315. doi:10.1016/j.ijheatmasstransfer.2017.10.111

Aoki, S. (1963). A consideration on the heat transfer in liquid metal. *Grafit-Gabrijel D.o.o.* doi:10.1016/S0016-5085(13)60330-3

Azer, N. Z., and Chao, B. T. (1961). Turbulent heat transfer in liquid metals-fully developed pipe flow with constant wall temperature. *Int. J. Heat Mass Transf.* 3 (2), 77–83. doi:10.1016/0017-9310(61)90069-2

Buhr, H. O., Carr, A. D., and Balzhiser, R. E. (1968). Temperature profiles in liquid metals and the effect of superimposed free convection in turbulent flow. *Int. J. Heat Mass Transf.* 11 (4), 641–654. doi:10.1016/0017-9310(68)90067-7

Chen, C. J., and Chiou, J. S. (1981). Laminar and turbulent heat transfer in the pipe entrance region for liquid metals. *Int. J. Heat. Mass Transf.* 24 (7), 1179–1189. doi:10.1016/0017-9310(81)90167-8

Chen, F., Huai, X., Cai, J., Li, X., and Meng, R. (2013). Investigation on the applicability of turbulent-Prandtl-number models for liquid lead-bismuth eutectic. *Nucl. Eng. Des.* 257, 128–133. doi:10.1016/j.nucengdes.2013.01.005

Cheng, X., and Tak, N. I. (2006). Investigation on turbulent heat transfer to lead–bismuth eutectic flows in circular tubes for nuclear applications. *Nucl. Eng. Des.* 236 (4), 385–393. doi:10.1016/j.nucengdes.2005.09.006

Cong, T., Wang, Z., Zhang, R., Wang, B., and Zhu, Y. (2021). Thermal-hydraulic performance of a pche with sodium and sco2 as working fluids. *Ann. Nucl. Energy* 157, 108210. doi:10.1016/j.anucene.2021.108210

Duponcheel, M., Bricteux, L., Manconi, M., Winckelmans, G., and Bartosiewicz, Y. (2014). Assessment of RANS and improved near-wall modeling for forced convection at low Prandtl numbers based on LES up to Reτ=2000. *Int. J. Heat. Mass Transf.* 75, 470–482. doi:10.1016/j.ijheatmasstransfer.2014.03.080

Groetzbach, G. (2003). "Turbulence modeling issues in ADS thermal and hydraulic analyses," in IAEA Technical Meeting on Theoretical and Experimental Studies of Heavy Liquid Metal Thermal Hydraulics, Karlsruhe, Germany, November 2003 (IAEA-TEC-DOC).

Guo, J., and Huai, X. (2013). Thermodynamic analysis of lead–bismuth eutectic turbulent flow in a straight tube. *Energy* 57 (1), 600–606. doi:10.1016/j.energy.2013.05.008

Huang, C., Cai, W., Wang, Y., Liu, Y., and Li, B. (2019). Review on the characteristics of flow and heat transfer in printed circuit heat exchangers. *Appl. Therm. Eng.* 153, 190–205. doi:10.1016/j.applthermaleng.2019.02.131

Ibragimov, M. K., Subbotin, V. I., and Ushakov, P. A. (1962). Investigation of heat transfer for turbulent flow of heavy liquid metals in tubes. *J. Nucl. Energy. Parts A/B. React. Sci. Technol.* 16 (3), 174–175. doi:10.1016/0368-3230(62)90094-0

Jaeger, W. (2016). Empirical models for liquid metal heat transfer in the entrance region of tubes and rod bundles. *Heat. Mass Transf.* 53 (5), 1667–1684. doi:10.1007/s00231-016-1929-8

Jaeger, W. (2017). Heat transfer to liquid metals with empirical models for turbulent forced convection in various geometries. *Nucl. Eng. Des.* 319, 12–27. doi:10.1016/j.nucengdes.2017.04.028

Jischa, M., and Rieke, H. B. (1979). About the prediction of turbulent Prandtl and schmidt numbers from modeled transport equations. *Int. J. Heat. Mass Transf.* 22 (11), 1547–1555. doi:10.1016/0017-9310(79)90134-0

Johnson, H. A., Hartnett, J. P., and Clabaugh, W. J. (1953). Heat transfer to molten lead-bismuth eutectic in turbulent pipe flow. *J. Fluids Eng.* 75 (6), 1191–1198. doi:10.1115/1.4015579

Kays, W. M. (1994). Turbulent Prandtl number—Where are we? *J. Heat. Transf.* 116 (2), 284–295. doi:10.1115/1.2911398

Kays, W. M., Crawford, M. E., and Weigand, B. (2004). *Convective heat and mass transfer*. New York: The McGraw-Hill Companies, Inc.

Kim, I., and Sun, X. (2014). CFD study and PCHE design for secondary heat exchangers withFLiNaK-Helium for SmAHTR. *Nucl. Eng. Des.* 270, 325–333. doi:10.1016/j.nucengdes.2014.02.003

Kim, I., Zhang, X., Richard, C., and Sun, X. (2016). Design study and cost assessment of straight, zigzag, S-shape, and OSF PCHEs for a FLiNaK–SCO2 Secondary Heat Exchanger in FHRs. *Ann. Nucl. Energy* 94, 129–137. doi:10.1016/j.anucene.2016.02.031

Kirillov, P. L., and Ushakov, P. A. (2001). Heat transfer to liquid metals: Specific features, methods of investigation, and main relationships. *Int. J. Heat. Mass Transf.* 48 (1), 50–59.

Li, H., Deng, T., Ma, T., Ke, H., and Wang, Q. (2019). A new evaluation method for overall heat transfer performance of supercritical carbon dioxide in a printed circuit heat exchanger. *Energy Convers. Manag.* 193, 99–105. doi:10.1016/j.enconman.2019.04.061

Liu, S., Jin, M., Lyu, K., Zhou, T., and Zhao, Z. (2018). Flow and heat transfer behaviors for double-walled-straight-tube heat exchanger of HLM loop. *Ann. Nucl. Energy* 120, 604–610. doi:10.1016/j.anucene.2018.06.016

Lyon, R. N. (1951). Liquid metal heat transfer coefficients. *Chem. Eng. Prog.* 47, 75–79. doi:10.1007/BF00412000

Marocco, Luca, and Garita, Francesco (2018). Large eddy simulation of liquid metal turbulent mixed convection in a vertical concentric annulus. *J. Heat. Transf.* 140 (7), 072504. doi:10.1115/1.4038858

Marocco, L., Valmontana, A., and Wetzel, T. (2017). Numerical investigation of turbulent aided mixed convection of liquid metal flow through a concentric annulus. *Int. J. Heat Mass Transf.* 105, 479–494. doi:10.1016/j.ijheatmasstransfer.2016.09.107

Menter, F. R. (1994). Two-equation eddy-viscosity turbulence models for engineering applications. *AIAA J.* 32 (5), 1598–1605. doi:10.2514/3.12149

Menter, F. R. "Zonal two equation k-w turbulence models for aerodynamic flows," in 24th Fluid Dynamics Conference, Orlando,FL,U.S.A, July 1993 (Reston: AIAA). doi:10.2514/6.1993-2906

Organisation For Economic Co-Operation And Development Nuclear Energy Agency (2015). *Handbook on lead-bismuth Butectic alloy and lead properties, materials Compatibility, thermal-hydraulics and Technologies*. OECD.

Pacio, J., Daubner, M., Fellmoser, F., Litfin, K., and Wetzel, T. (2016). Experimental study of heavy-liquid metal (LBE) flow and heat transfer along a hexagonal 19-rod bundle with wire spacers. *Nucl. Eng. Des.* 301, 111–127. doi:10.1016/j.nucengdes.2016.03.003

Pidaparti, Sandeep R., Anderson, Mark H., and Ranjan, Devesh (2019). Experimental investigation of thermal-hydraulic performance of discontinuous fin printed circuit heat exchangers for supercritical CO2 power cycles. *Exp. Therm. Fluid Sci.* 106, 119–129. doi:10.1016/j.expthermflusci.2019.04.025

Reynolds, A. J. (1975). The prediction of turbulent Prandtl and schmidt numbers. *Int. J. Heat. Mass Transf.* 18 (9), 1055–1069. doi:10.1016/0017-9310(75)90223-9

Roelofs, F., Gerschenfeld, A., Tarantino, M., Tichelen, K., and Pointer, W. D. (2019). "Thermal-hydraulic challenges in liquid-metal-cooled reactors-sciencedirect," in *Thermal Hydraulics aspects of liquid metal cooled nuclear reactors*, 17–43. doi:10.1016/B978-0-08-101980-1.00002-8

Saeed, M., and Kim, M. H. (2017). Thermal and hydraulic performance of SCO2 PCHE with different fin configurations. *Appl. Therm. Eng.* 127, 975–985. doi:10.1016/j.applthermaleng.2017.08.113

Skupinski, E., Tortel, J., and Vautrey, L. (1965). Determination des coefficients de convection d'un alliage sodium-potassium dans un tube circulaire. *Int. J. Heat Mass Transf.* 8 (6), 937–951. doi:10.1016/0017-9310(65)90077-3

Sleicher, C. A., Awad, A. S., and Notter, R. H. (1973). Temperature and eddy diffusivity profiles in NaK. *Int. J. Heat. Mass Transf.* 16 (8), 1565–1575. doi:10.1016/0017-9310(73)90184-1

Stromquist (1953). *Effect of WETTING on heat transfer characteristics of liquid metals*. [Tennessee Univ]. The University of Tennessee. [Technical Report].

Subbotin, V. I., Papovyants, A. K., Kirillov, P. L., and Ivanovskii, N. N. (1963). A study of heat transfer to molten sodium in tubes. *Soviet J. Atomic Energy* 13 (4), 991–994. doi:10.1007/BF01480861

Thiele, R., and Anglart, H. (2013). Numerical modeling of forced-convection heat transfer to lead–bismuth eutectic flowing in vertical annuli. *Nucl. Eng. Des.* 254, 111–119. doi:10.1016/j.nucengdes.2012.09.006

Wang, C., Wang, C., Zhang, Y., Zhang, D., Tian, W., Qiu, H., et al. (2021). Investigation on flow heat transfer characteristic of lead-bismuth eutectic alloy. *Atomic Energy Sci. Technol.* 55 (5), 822–828. doi:10.7538/yzk.2020.youxian.0356

Wang, Y., Li, X., Huai, X., Cai, J., and Xi, W. (2017). Experimental investigation of a lbe-helium heat exchanger based the ads. *Prog. Nucl. Energy* 99, 11–18. doi:10.1016/j.pnucene.2017.04.013

Xu, J., Liu, C., Sun, E., et al. (2020). Review and perspective of supercritical carbon dioxide power cycles. *Therm. Power Gener.* 49 (10), 1–10. doi:10.19666/j.rlfd.202004089

Zhang, J., Kapernick, R. J., Mcclure, P. R., and Trapp, T. J. (2013). Lead-bismuth eutectic technology for hyperion reactor. *J. Nucl. Mater.* 441 (1-3), 644–649. doi:10.1016/j.jnucmat.2013.04.079

Zhang, Y., Wang, C., Lan, Z., Wei, S., Chen, R., Tian, W., et al. (2020). Review of thermal-hydraulic issues and studies of lead-based fast reactors. *Renew. Sustain. Energy Rev.* 120, 109625. doi:10.1016/j.rser.2019.109625

Zhao, P., Zhu, J., Ge, Z., Liu, J., and Li, Y. (2018). Direct numerical simulation of turbulent mixed convection of LBE in heated upward pipe flows. *Int. J. Heat. Mass Transf.* 126, 1275–1288. doi:10.1016/j.ijheatmasstransfer.2018.05.104

Zhu, F., Junmei, W. U., Shi, L., and Guanghui, S. U. (2019). Experimental study on flow and heat transfer characteristic of liquid lead-bismuth eutectic in annular channel. *Atomic Energy Sci. Technol.* 53 (5), 819–825. doi:10.7538/yzk.2018.youxian.0495

Nomenclature

c_p specific heat
G mass flux
h enthalpy
k thermal conductivity; turbulent kinetic energy
Pr Prandtl number
p pressure
Pe Peclet number
Re Reynolds number
T temperature
u velocity
y distance from wall

Greek symbols

μ viscosity
ν kinematic viscosity
ω specific dissipation rate
ρ density
ε turbulence dissipation rate

Superscripts and subscripts

k turbulent kinetic energy
t turbulent
ω specific dissipation rate